Journal of the European Ceramic Society 20 (2000) 1947–1957

Electrical conductivity measurements as a microprobe for structure transitions in polysiloxane derived Si–O–C ceramics

Jens Cordelair, Peter Greil *

University of Erlangen-Nuernberg, Department of Materials Science (Glass and Ceramics), Martensstr. 5, D-91058 Erlangen, Germany

Received 29 September 1999; received in revised form 4 February 2000; accepted 12 February 2000

Abstract

Polysiloxanes $[RSiO_{1.5}]_n$ with $R = CH_3$ (PMS) and C_6H_5 (PPS), respectively, were transformed to Si–O–C ceramics of variable composition and structure upon pyrolysis in inert atmosphere at 800–1500°C. The electrical conductivities of the Si–O–C ceramics in air were measured at room temperature by using a shielded two point configuration. In situ measurements of the dc-conductivity during the pyrolytic conversion from the polymer to the ceramic phase were carried out up to 1500°C with four point contacted carbon electrodes in inert atmosphere. During polymer-ceramic conversion excess carbon precipitates above 400°C (PPS)–700°C (PMS). At temperatures above 800°C (PPS) and 1400°C (PMS) coagulation and growth of the carbon clusters results in a percolation network formation. While below the percolation threshold electrical conductivity can be described according to Motts mechanism by variable-range-hopping of localized charge carriers, regular electron band conduction due to the instrinsic conductivity of turbostratic carbon (8×10^{-4} $(\Omega\text{cm})^{-1}$) predominates above. Thus, the in situ measurement of non-linear electrical property changes can be used as a microprobe of high sensivity to detect microstructural transformations during the pyrolysis of preceramic polymers.

Keywords: Carbon; Electrical conductivity; Percolation network; Precursors-organic; Si–O–C

1. Introduction

Ceramics with an amorphous or nanocrystalline microstructure are obtained when preceramic polymers such as poly(carbosilane), -(silazane), -(siloxane), etc. are pyrolysed at temperatures above 600–800°C in inert atmosphere.[1–5] Cleavage of chemical bonds between silicon and various functional groups gives rise to volatilization of organic fragments. The low density organic polymer structure transforms to a metastable inorganic network structure (amorphous residue) of substantially higher density which may crystallize into multiphase ceramic materials at temperatures above 1000–1400°C. Due to the tailorability of their structure on a molecular scale preceramic polymers have become a matter of increasing research efforts[6] for the development of novel ceramic materials such as high temperature resistant ceramic fibers, wear resistant coatings, low density insulating foams, advanced joining systems, etc. Using preceramic polymers as advanced reaction binders in powder systems low temperature processing becomes possible[7] which may be of particular benefit for net shape manufacturing of complex shaped components as well as for new solid free form fabrication techniques.[8]

Among the phases occuring in the polymer derived Si–C, Si–O–C, Si–C–N, Si–O–C–N and Si–B–N–C materials SiO_2, BN, and Si_3N_4 are insulators ($\sigma_{dc}(RT) = 10^{-14} - 10^{-12}(\Omega\text{cm})^{-1}$) whereas SiC, amorphous carbon (a-C) and $Si_xC_yN_z$ are semiconductors ($\sigma_{dc}(RT) = 10^{-4} - 10^{2}(\Omega\text{cm})^{-1}$). Turbo stratic carbon and graphite have a significantly higher conductivity ($\sigma_{dc}(RT) = 1 - 10^{5}(\Omega\text{cm})^{-1}$). The conductivity of amorphous semiconducting materials is influenced by the presence of dangling bonds (unsaturated bonds) which give rise to midgap-states in the band gap of the amorphous semiconductor.[9] Temperature dependence of amorphous semiconductors at low temperatures was found to follow

$$\sigma_{dc}(T) \sim \exp\left(-\frac{T_o}{T^{1/4}}\right) \qquad (1)$$

---

* Corresponding author.

E-mail address: greil@ww.uni-erlangen.de (P. Greil).

0955-2219/00/$ - see front matter
PII: S0955-2219(00)00068-6

which describes the variable range hopping mechanism as derived by Mott.[10] At high temperatures,

$$\sigma_{dc}(T) \sim \exp\left(-\frac{E^*}{kT}\right) \tag{2}$$

is associated with tunneling of charge carriers between excited states as well as excitation into the conduction band resulting in an Arrhenius type of temperature dependence of the electrical conductivity.[11]

Amorphous a-SiCN and a-SiBCN pyrolysis products of poly(silazanes) and poly(borosilazanes), respectively, were found to behave as electron semiconductors following Eq. (1) over a wide range of temperatures.[11,12] Large polarons with overlapping wave functions represent the major charge carriers the formation of which might be facilitated by the high degree of disorder in the polymer derived residue.[11] Crystallization of the amorphous polymer residue phase at elevated temperatures results in an increase of the conductivity by several orders of magnitude due to the formation of an interconnected percolation network of SiC or C. In fact, it was found that any of the materials prepared from Si–C, Si–C–N, Si–C–O and Si–C–N–O precursor polymers developed a free carbon phase even for C/Si-ratios as low as 0.7.[13] dc-Conductivity of polycrystalline materials was found to follow Eq. (2) and a distinct effect of the grain boundaries could be confirmed. Carbon content and interconnectivity of the carbon network was identified to exert a major influence on the electrical properties.[13–17] High fractions of carbon with sp^2-hybridization result in high conductivities of the pyrolyzed materials. The ratio of sp^2 to sp^3 bonding of the carbon species was associated with the residual hydrogen content which depends on the polymer composition as well as on the pyrolysis conditions e.g. temperature, atmosphere. Thus the ectrical conductivity σ_{dc}(rt) measured at room temperature can be varied in a wide range (Si–C–O): 10^{-13}–$10^{-1}(\Omega\text{cm})^{-1}$,[15–17] Si–C–N: 10^{-15}–$10^{0}(\Omega\text{cm})^{-1}$,[11] Si–B–C–N: 10^{-7}–$10^{1}(\Omega\text{cm})$.[11]

This large variation of the electrical conductivity and its sensitivity to the carbon distribution during processing offers the possibility to use the electrical property changes as an internal microprobe for microstructure transformations during pyrolysis. Detection of carbon redistribution reactions serves as a highly sensitive tool to analyze rearrangement, phase separation, crystallization etc. during thermal treatment of polymeric precursor systems. As a model system two poly(siloxanes) $[RSiO_{1.5}]_n$ with different carbon content were investigated. Highly crosslinked poly(siloxanes) with R = alkyl-, aryl-, vinyl-groups etc. and $n \gg 100$ are obtained by controlled hydrolysis-condensation of chloro- or alkoxy-silanes of mean functionality greater than two (R_2SiCl_2, $RSiCl_3$). While the oxygen content limits their use as precursor materials for ceramics to be applied at temperatures below 1200°C (at higher temperatures carbothermal reduction by elementary C or SiC[18]

$$\begin{aligned} SiO_2(s) + C(s) &\rightarrow SiO(g) + CO(g) \\ 2SiO_2(s) + SiC(s) &\rightarrow 3SiO(g) + CO(g) \\ SiO_2(s) + 3C(s) &\rightarrow SiC(s) + 2CO(g) \end{aligned}$$

results in extended porosity formation) they offer attractive advantages: industrial availability, non-toxic decomposition products, stability in air and humid atmospheres as well as a high ceramic yield of more than 90 wt%. Recently, poly-(siloxanes) have received attention as precursor materials for ceramics such as silicon carbide and silicon oxycarbide (SiOC) from which ceramic fiber composites, coatings, joinings and foams were made.[19–24]

Pyrolysis in inert atmosphere generally involves several distinct steps:[17,25] (i) an organometallic–inorganic transition between 500 and 800°C, leading to an amorphous hydrogenated solid a-SiOCH built on tetrahedral structures of the type $Si(O_aC_b)$ with $a+b=4$, depending on the inital polymer composition; (ii) nucleation of clusters of excessive carbon generally as so-called basic structural units (BSUs) which are small stacks of 2–3 polyaromatic layers (graphenes)[13] above 800°C and (iii) precipitation of nanocrystals of SiO_2 and SiC at temperatures between 1200 and 1600°C. Grain coarsening results in consumption of the residual amorphous phase and reduction of oxygen content due to a probable evaporation of SiO and CO. The formation of a continous network of polyaromatic, turbostratic carbon results in a sharp insulator-quasi metal transition. The percolation threshold depends on the carbon content in the polymer precursor and the processing conditions. A pore phase is also present at 5–20 vol% with glo- bular nanopores of 1–50 nm.[26] The average pore size increases and volume fraction of porosity decreases with increasing pyrolysis temperature, resulting in irreversible shrinkage (densification) on heating the ceramic residue above the maximum pyrolysis temperature.

In the present paper electrical conductivity measurements on two poly(siloxanes), a methyl- and a phenyl-containing polymer, which differ in the carbon content of 17–45 wt%, respectively, will be reported. An in situ dc-conductivity measurement technique was developed which allows to monitor the conductivity changes during the organometallic–inorganic transition upon heating. Thermal balance as well as IR, Raman and EPR spectroscopy techniques were applied to analyze the structural transformations from the amorphous a-SiOCH to the crystalline material which consists of SiO_2, C and SiC, respectively. Among the variety of different statistical, geometrical and thermodynamic models to explain electrical conductivity of phase mixtures[27] general effective

Table 1
Characteristics of the poly(siloxanes) PMS and PPS

Polymer	Poly(phenylmethylvinylhydrogensiloxane) PPS	Poly(methylhydrogensiloxane) PMS
Composition	$RSiO_{1,5}$ $R=[(C_6H_5)_{2,8},(CH_3)_{1,5},(CH_2{=}CH), (H)]$ liquid	$RSiO_{1,5}$ $R=[(CH_3)]$ powder
Producer	Wacker Germany	Nuenchritz Germany
Polymerisation mechanism	Polyaddition	Polycondensation
Solvent	Isopropanol, Aceton	Isopropanol, Aceton
Density (23°C) (kg m^{-3})	1,1-1,15	1,1-1,31
Melting point (°C)	RT liquid	$\geqslant 45$
Kinematic viscosity (23°C) (m^2 s^{-1})	$1.4\times10^{-3}\pm4\times10^{-4}$	Powder
Shelf life (23°C)	12 Months	Unlimited

media (GEM) theory[28] was used to fit electrical conductivity as a function of the volume fractions of the non-conducting matrix (SiO_2) and the conducting inclusion phase (SiC, C).

2. Experimental procedure

2.1. Specimen preparation

A methyl-containing poly(siloxane) (PMS) (NH2100, Huels AG, Marl, Germany) of low carbon content (17 wt%) and a phenyl-containing poly(siloxane) (PPS) (H62C, Wacker Chemie, Burghausen, Germany) of high carbon content (45.5 wt%) were used as polymer precursor materials. Table 1 summerizes the material data as provided by the suppliers. The PMS contains silanol groups which undergo a condensation reaction upon heating above 150°C resulting in the release of H_2O. Curing reaction of PPS is governed by a hydrosilation reaction (β-addition) via vinyl groups at similar temperatures.

Disks (diameter 25 mm, height 3 mm) and bars ($2\times4\times50$ mm^3) were prepared for the electrical measurements. While the PMS powder was cured in a thermo-press at 250°C for 3 h applying an uniaxial pressure of 20 MPa the PPS liquid was pressureless cured in Teflon dies at 230°C for 4 h.

2.2. Electrical dc-conductivity measurements

In situ measurements of the electrical resistance during pyrolysis from room temperature to 1500°C were conducted in an electrically heated alumina tube furnace in Ar atmosphere. Temperature at the specimen site was controlled using an encapsulated Pt–PtRh thermocouple. Resistance measurements at temperatures below 1000°C (high resistance regime) were conducted in a shielded two point configuration with an ammeter (6162, Keithley, Munich, Germany) using thin pellets. The pellets were coated with conducting carbon to achieve electrical contact with the carbon electrodes pressed on the samples. Above 1000°C (low resistance regime) a four point configuration was applied using a multifunctional resistance analyzer (2010, Keithley, Munich, Germany). Molybdenum wires were fixed on the rectangular specimen with tungsten paste at 1000°C. The electronic conductivities of samples were measured by dc-circuit at 50–300 V. Both measurement configurations were integrated in specially designed carbon holders, Fig. 1.

2.3. Microstructure analysis

Weight loss upon pyrolyis was examined by heating compacted specimens in a thermal balance (STA 409, Netzsch Geraetetechnik, Selb, Germany) in flowing Ar atmosphere with a constant heating rate of 5°C/min. The bulk densities of the pyrolyzed samples were measured by the Archimedian method, using distilled water. The open porosity was determined by high pressure mercury intrusion (Porosimeter 2000, Carlo Erba, Rodano, Italy).

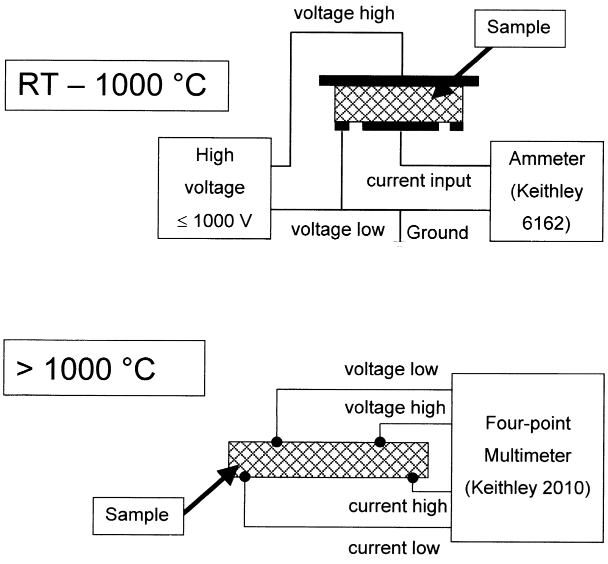

Fig. 1. Experimental set up of in situ electrical dc-measurements in the low temperature regime from RT to 1000°C (top) and in the high temperature regime from 1000 to 1500°C (bottom).

Thermal degradation and release of organofunctional groups of the polymers was examined by FTIR (420, Nicolet, Madison, US) in the range 450–4000 cm^{-1} with a resolution of 1 cm^{-1}. Compact specimens were measured in diffusive reflectance mode and the following vibration bands were observed (wave number in 1/cm): (Si–O–Si) 1000–1100, (Si–CH_3) 800, (Si–C_6H_5) 1275, (C=C) 1600, (Si–H) 2160, (C–H_3) 2900, and (C–H) 3060.

The state of hybridization of carbon e.g. sp^3 and sp^2 was characterized by Raman spectroscopy using the vibration bands at 1330 and 1580 cm^{-1}. The Raman-spectra (Ramascope 2000, Renishaw, Gloucestershire, GB) were counted with a laser at 514 nm and a lateral resolution of 1 cm^{-1}.

The precipitation of carbon clusters was analyzed by EPR spectroscopy. 10 mg of powdered sample was examined in a X-band spectrometer (ESP300, Bruker, Rheinstetten, Germany). The operation frequency was 9.5 GHz with a modulation of 100 kHz. The relative number of paramagnetic spins $N = I(\Delta H)^2$ was calculated from the signal intensity for carbon at 3450×10^{-4} T (Landé factor g = 2.003), I, and the line width, ΔH.[29] High resolution TEM (EM 400 T, Philips, Eindhoven, NE) of ion thinned specimens at an acceleration voltage of 40 kV was used to visualize the microstructure of the carbon network which was supposed to have fully developed after pyrolysis at 1400°C.

3. Results

Fig. 2 shows the weight loss resulting from thermal degradation of the two polysiloxanes during heating. Total weight losses of PMS and PPS at 1200°C are 15.9 and 27.4 wt%, respectively. Chemical analysis reveals a total carbon content in the ceramic residue of 14.5 wt% (PMS) and 41.1 wt% (PPS) at 1400°C, respectively, indicating a carbon loss due to evaporation of 2.5 wt% (PMS) and 4.4 wt% (PPS). Assuming SiO_2, SiC and C to be the only thermodynamically stable phases, the elemental anlysis data can be attributed to the following phase compositions (in wt%, pyrolysed in argon at 1400°C) which was confirmed by a thermal barometric analysis technique:[30] PMS (69.3 SiO2, 23.1 SiC, 7.6 C) and PPS (40.1 SiO2, 26.8 SiC, 33.1 C).

As may be concluded from the weight loss rate curves, cleavage of Si–(C_6H_5) bonds and release of C_6H_6 is the dominating degradation reaction between 300 and 600°C (PPS) whereas cleavage of Si–(CH_3) bonds and volatilization of CH_4 (PMS) prevails between 600 and 800°C. At higher temperatures dehydrogenation still occurs resulting only in a minor weight reduction up to 1200°C (above this temperature carbothermal reduction $SiO_2 + C \rightarrow SiO + CO$ may result in further weight loss).

Fig. 3 shows the results of FTIR measurements in the temperature range between 400°C and 900°C where the organic–inorganic transition occurs. Realease of methane due to cleavage of Si–C(H_3) bonds in PMS, Fig. 3a, is observed above 600°C and almost terminated at 700°C. A maximum of newly formed Si–H bonds occurs at 800°C. In PPS, Fig. 3b, cleavage of the functional group Si–C_6H_5 can be observed at lower temperatures (> 400°C) whereas C=C double bonds from the vinyl groups remain stable up to > 800°C.

As a result of the release of organic fragments the character of the residue changes from an organic network to an inorganic solid which is associated with a substantial increase of the density, Fig. 4. Mercury

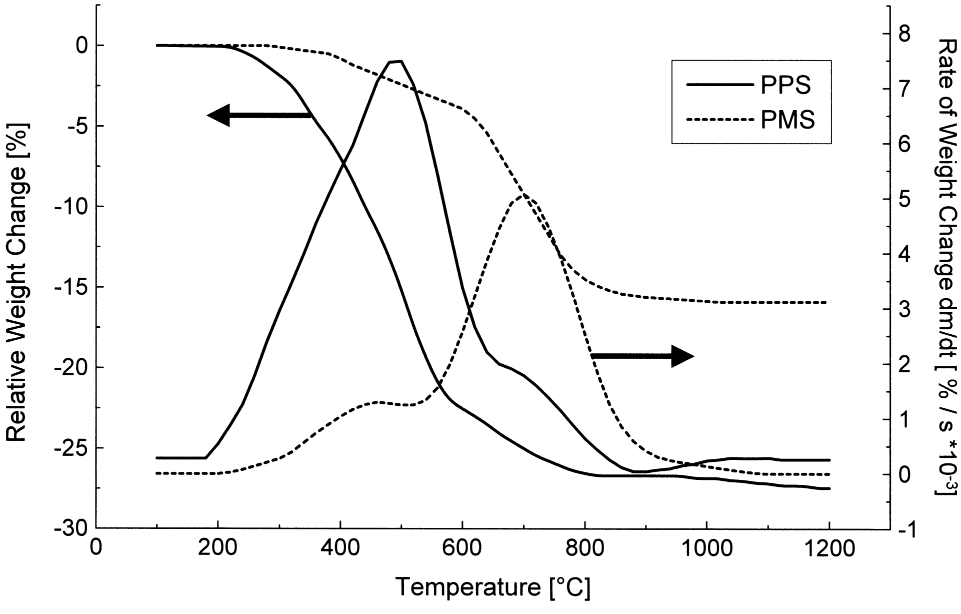

Fig. 2. Relative weight loss and rate of weight loss versus temperature at a constant heating rate of 5°C/mm in Ar-atmosphere.

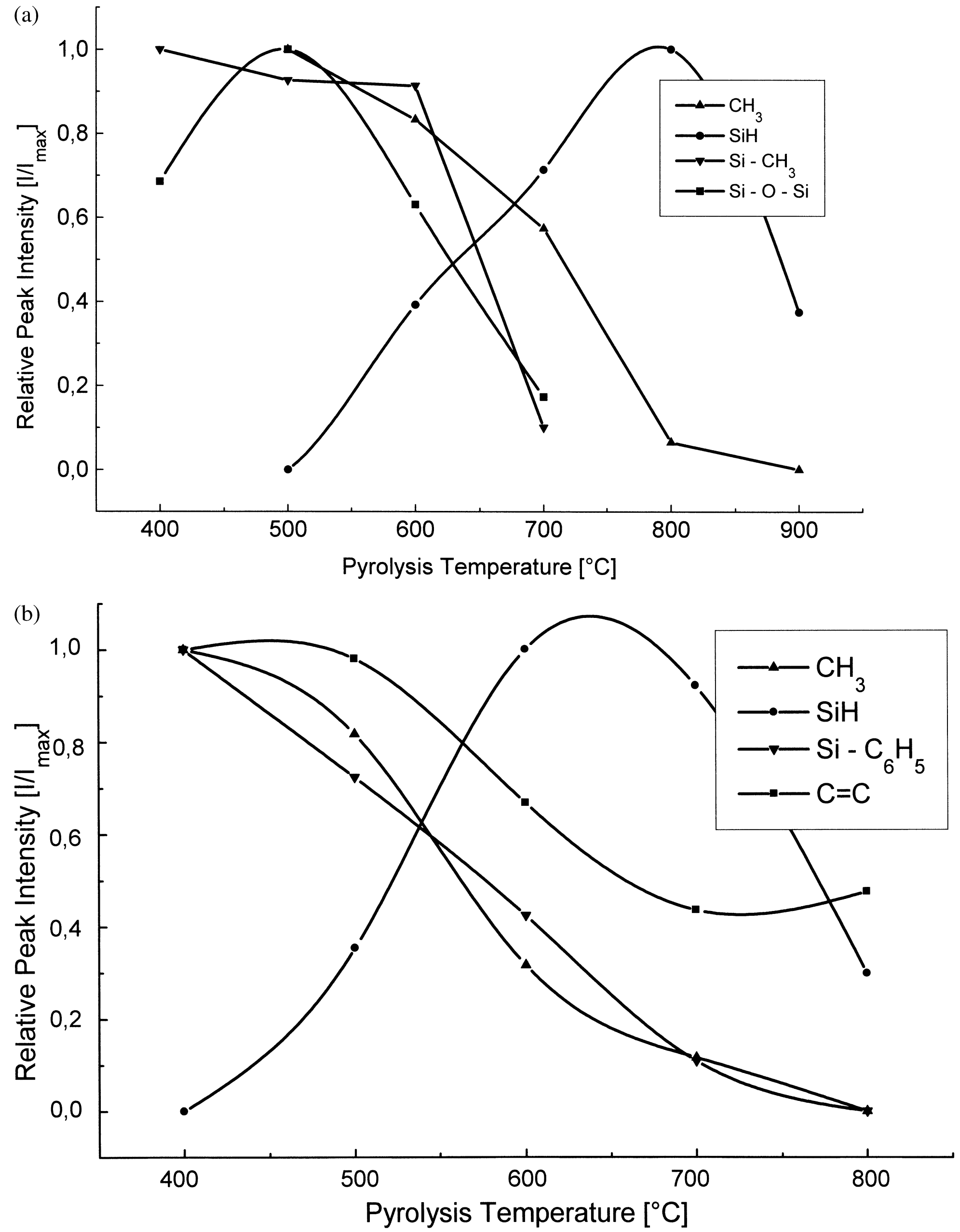

Fig. 3. Relative IR-peak intensities (normalized to the maximum intensity I_{max}) of (a) PMS and (b) PPS after pyrolysis.

intrusion measurements confirm the formation of a large transient open porosity in the temperature range where thermal degradation occurs. The interconnected pore network is necessary as a pathway for the release of the volatile decomposition products.

Eliminination of transient porosity due to viscous flow and sintering at temperatures above 800°C indicates the transition to the inorganic a-SiOC(H) network (Si–H vibrations in the IR spectra still show the presence of some hydrogen). Porosity elimination and density increase give rise for an extended volume change resulting in a large linear shrinkage of up to more than 30% which makes it difficult to manufacture bulk components from preceramic polymers. Incorporation of particulate fillers, however, could be successfully used to compensate for part of the polymer shrinkage so that bulk component manufacturing becomes accessible,[7] Depending on the electrical properties of the fillers and their connectivity (determined by particle size and volume fraction) conductivity of the polymer/filler derived ceramics may be tailored in a wide range.[31]

While thermogravimetric analysis, density and porosity measurements provide a picture of the overall microstructural changes that are associated with the polymer pyrolysis, electrical conductivity measurements during the pyrolysis (in situ measurements) are more sensitive to detect structural rearrangement reactions such as phase separation, precipitation, network formation, etc. Fig. 5 shows the change of dc-conductivity from room temperature to 700°C and Fig. 6 from 1000°C to 1500°C. Both poly(siloxane) polymers exhibit insulating behavior at room temperature $\left(\sigma_{\mathrm{rt}} \leqslant 10^{-12} (\Omega\mathrm{cm})^{-1}\right)$. Generally, the conductivity increases upon heating resulting in an insulator-conductor transition after the polymer-ceramic conversion is completed above 1400°C (PMS: $\sigma_{1400°\mathrm{C}} \geqslant 10^{-2} (\Omega\mathrm{cm})^{-1}$; PPS: $\sigma_{1400°\mathrm{C}} \geqslant 10^{0} (\Omega\mathrm{cm})^{-1}$). Both polymers show nonlinearities in the low temperature regime of the conductivity-temperature curves at 430–530°C (PMS) and at 300–320°C and 480–500°C (PPS), respectively, which indicate chain rupture due to bond cleavage. In the high temperature regime PMS exhibits another nonlinear increase of conductivity at approximately 1300°C when the carbon precipitations form a percolation network.

EPR spectra obtained from pyrolysed specimens reveal the formation of elemental carbon in PPS even at 400°C whereas in PMS temperatures above 700°C are needed. Fig. 7 shows the total EPR spin density of both polymers versus the pyrolysis temperature. Above 800°C both polymers exhibit almost the same concentration of

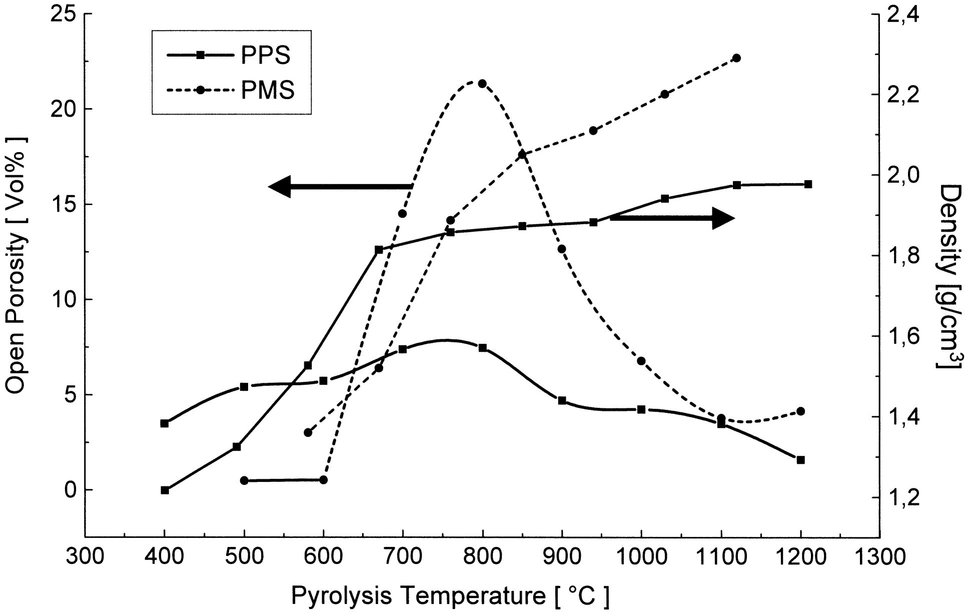

Fig. 4. Open (transient) porosity and density versus temperature during heating with a constant heating rate of 5°C/min in Ar-atmosphere.

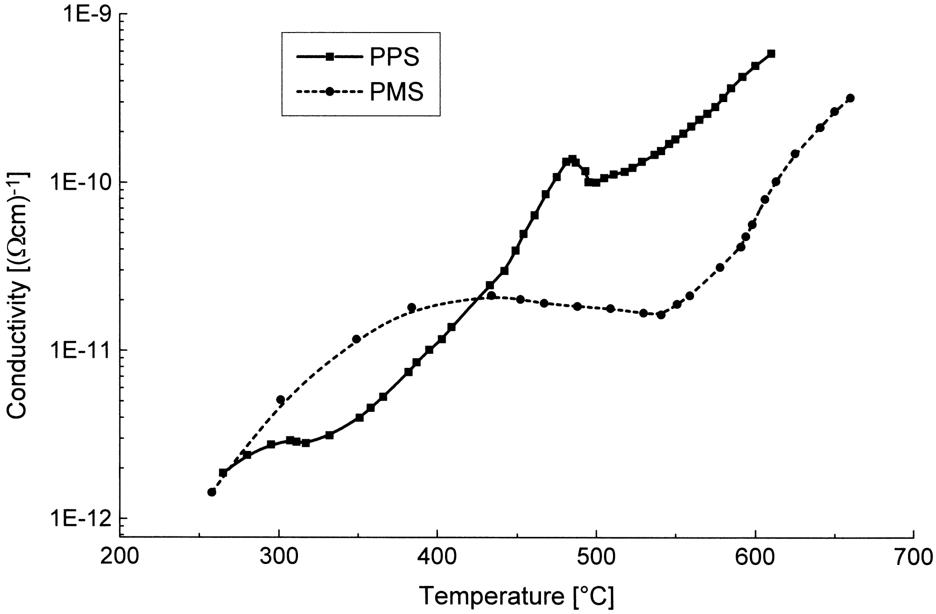

Fig. 5. In situ electrical dc-measurements from room temperature to 700°C.

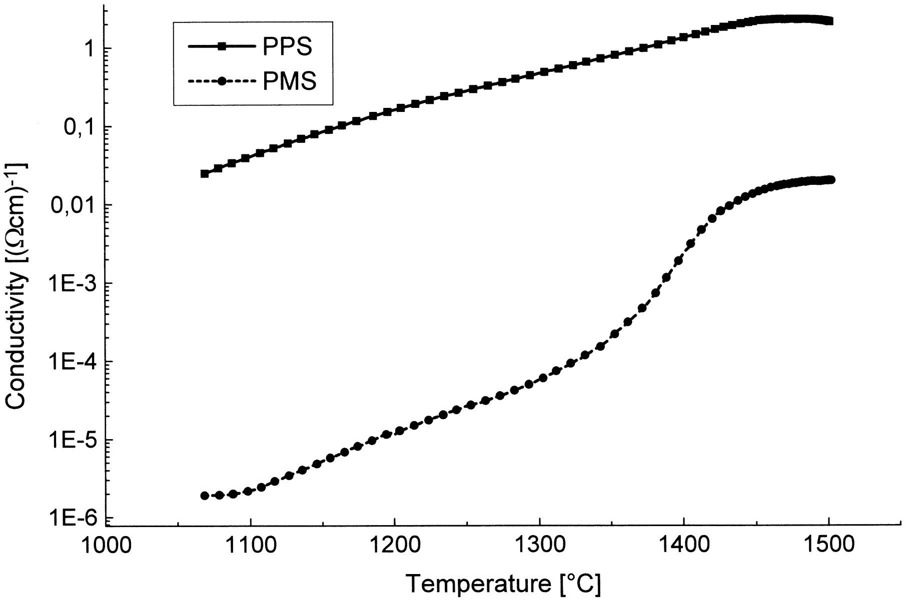

Fig. 6. In situ electrical dc-measurements from 1000 to 1500°C.

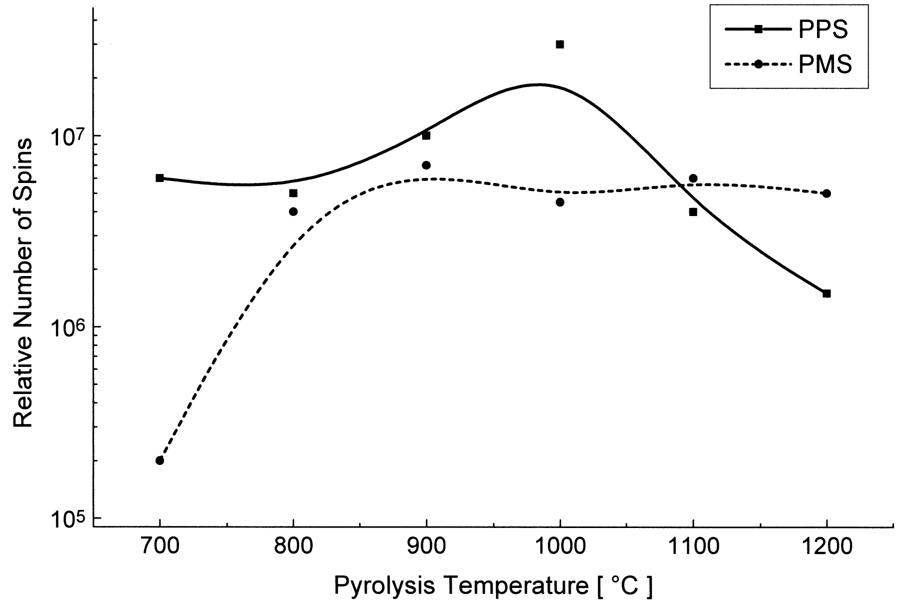

Fig. 7. EPR-spin densities of carbon versus pyrolysis temperature.

paramagnetic centers associated with precipitation of carbon even though the total carbon content is different.

Raman spectra were taken to analyze the type of carbon hybridization. Fig. 8 shows the ratio of C-sp^3 to C-sp^2 in the temperature range from 900 to 1600°C. Above 1100°C the bonding character of carbon precipitated from PPS changes from sp^3 to sp^2 which indicates the formation of carbon with a turbostratic structure of aromatic carbon sheets (BSU).[32] TEM analyses clearly show the morphology of the turbo-stratic carbon forming an interconnected network after pyrolysis at 1400°C, Fig. 9. While the thickness of the carbon ribbons are similar in both polymer derived residues (approximately 80 nm) the network density (e.g. the mean distance between the ribbons) is significantly higher in the carbon rich PPS derived material.

4. Discussion

After reaching the thermal decomposition temperature, bond rupture at 300°C (Si–C–C–Si from hydrosilation curing reaction) and 500°C (Si–O–Si) gives rise for the nonlinearities observed in the conductivity ver-

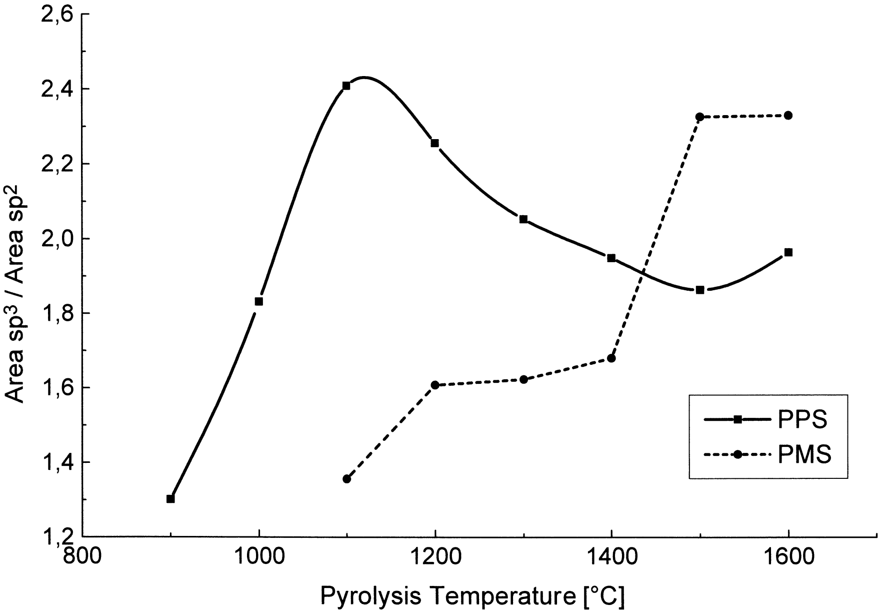

Fig. 8. Ratio of C-sp^3/C-sp^2 Raman intensities versus pyrolysis temperature.

sus temperature curves, Figs. 5 and 6. In analogy to Peierls instabilities in one-dimensional conducting systems thermally induced bond rupture affects conduction via localised electron states along the macromolcular polymer chains. A variety of decomposition reactions involving cleavage of Si–C and Si–O bonds and formation of radicals have been described to occur in poly(siloxanes):[33,34]

$$[\mathrm{Si-OH}] + [\mathrm{H_3C-Si}] \rightarrow [\mathrm{Si-O-Si}] + \mathrm{CH_4}$$
$$[\mathrm{Si-OH}] + [\mathrm{H_5C_6-Si}] \rightarrow [\mathrm{Si-O-Si}] + \mathrm{C_6H_6}$$
$$[\mathrm{Si}] + [\mathrm{H-C}] \rightarrow [\mathrm{Si-H}] + [\mathrm{C}\bullet]$$
$$[\mathrm{Si-O}] + [\mathrm{H-C}] \rightarrow [\mathrm{Si-OH}] + [\mathrm{C}\bullet]$$

Decomposition of hydrocarbon fragments resulting from cleavage of the functional groups bonded to silicon (Si–C_6H_5 and Si–CH_3) results in the precipitation of clusters of aromatic carbon in PPS above 400°C and of homogeneously distributed carbon in PMS above 600°C, respectively. Hydrogen is usually bondend to the periphery of the BSUs.[13] Removal of hydrogen is related to an increase in the number of free radicals due to the rupture of C–H side-bonds in the carbonaceous phase.[16] Formation of [C•] radicals with unsaturated electrons are supposed to give rise for the EPR signals at 0.03450 T ($g = 2.003$) observed above 600°C.[29] With increasing temperature the clusters of turbostratic carbon grow[17] and may coalesce by edge-to-edge linkage of neighboring BSUs[13] to form an interconnected network (cluster size to infinity) of turbostratic carbon above 800°C in PPS and 1400°C in PMS, respectively. In the polyaromatic carbon network nanometer size SiC crystals were found to be inserted as within uncomplete carbon cages.[13] Fig. 10 summerizes a model of the major structural transitions during heating of the two pol(siloxane) precursors.

From various results presented in literature, conduction dominated by direct particle–particle contact has been found when the materials were filled with large particles (larger than 0.1 µm, short carbon fibers).[35] On the other hand, tunneling conduction has been discussed when particles are very small (less than 0.1 µm). Depending on their size, particles involved in conducting aggregates or clusters either make direct contact (percolation regime) or remain at finite distances from one another (tunneling regime). The semiconducting behavior in the tunneling regime [room temperature to 800°C (PPS), 1400°C (PMS)] is attributed to thermal fluctuation-induced tunneling of electrons among evenly distributed charge carrier clusters, the temperature dependence of which is described by Eq. (2). An important conclusion from experimental observation in carbon black filled polymers[35] was that the tunneling junction characteristics (width, potential barrier) remain independent of filler concentration. In contrast the conductivity in the percolation regime at higher temperatures depends on the concentration of carbon clusters e.g. the distance between the particles in the macroscopic conductivity is a function of particle size and concentration.

Conductivity in the percolation regime above the critical temperatures where a continous network of carbon could form may be described using general effective media theory, GEM. GEM, which combines most apects of both percolation and effective media theories predicts the percolation transition in a continous media near the insolator-conductor transition[36] as a function of volume fraction Φ of the high conductivity phase e.g.

carbon in a matrix of low conductivity e.g. SiOC(H). The mean conductivity σ_m of a composite material which consists of a high (h) and a low (l) conducting phase with finite values for σ_h and σ_l is given as[37]

$$\frac{(1-\Phi)\left(\sigma_l^{1/t}-\sigma_m^{1/t}\right)}{\sigma_l^{1/t}+A\sigma_m^{1/t}}+\frac{\Phi\left(\sigma_h^{1/t}-\sigma_m^{1/t}\right)}{\sigma_h^{1/t}+A\sigma_m^{1/t}}=0 \qquad (3)$$

The constant A is a function of the critical volume fraction Φ_c of the high conductivity phase

$$A=\frac{1-\Phi_c}{\Phi_c} \qquad (4)$$

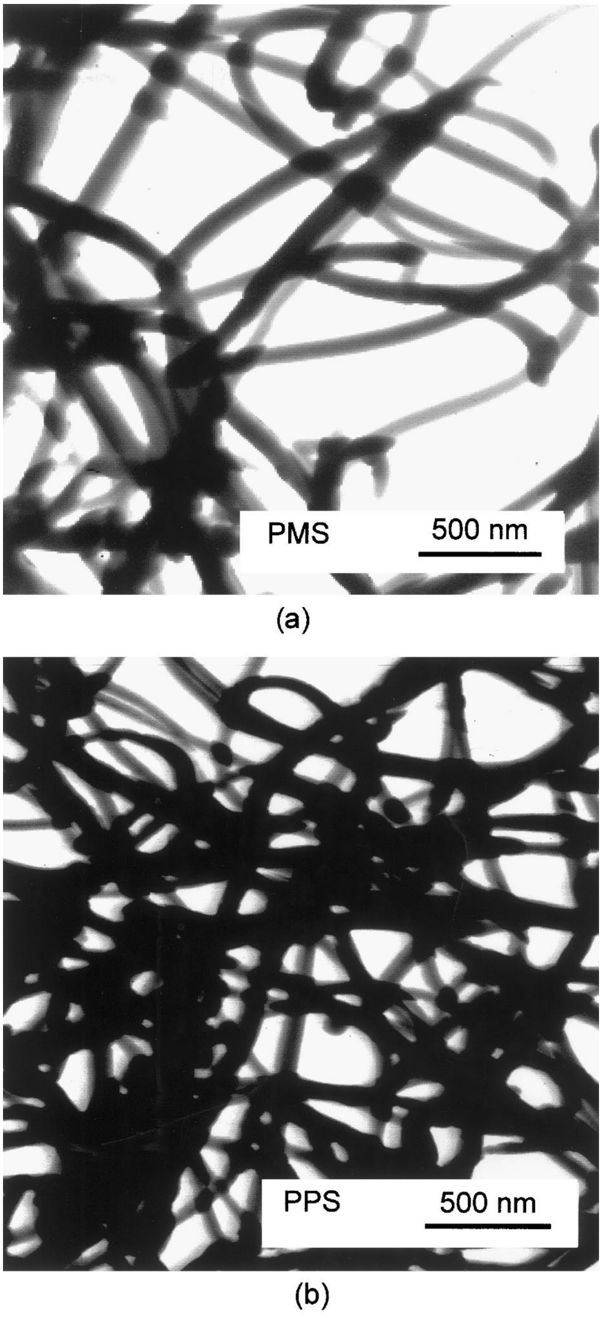

Fig. 9. TEM-micrographs of turbostratic carbon network formation in (top) PMS and (bottom) PPS after pyrolysis at 1400°C.

Although the value for the morphology parameter t for composites is most often found to lie in the range of 1.65–2.0 signficantly higher values up to 3.1 were found for graphite (flaky) particles in polymers.[38] Such high values of t were related to tunneling processes between the conducting particles.[39] Percolation threshold, Φ_c, was found to depend on the shape of the high conductivity cluster particles and typically varies between 0.01 and 0.6 in composite materials.[28] Monte Carlo studies of the percolation threshold in conducting fiber like particles containing insulating polymers showed that the higher the aspect ratio of the fibers the lower the critical volume fraction for onset of percolation.[40] For short fiber containing composites a percolation threshold below 5 vol% was estimated when the aspect ratio exceeds 100.[41] Though PMS exhibits a much lower content of free carbon (7.6 wt%/9 vol%) than PPS (33.1 wt%/37.8 vol%) an extended growth morphology of ribbon like carbon clusters may well exceed this percolation threshold.

Assuming typical values for $\sigma_l(SiO_2) \approx 10^{-14}(\Omega cm)^{-1}$, $\sigma_h(C) \approx 10^4(\Omega cm)^{-1}$[11] the mean composite conductivity σ_m was calculated as a function of the volume fraction of high conductivity phase Φ according to Eq. (3) for different values of t, Fig. 11. To account for the influence of carbon particle morpholgy, the percolation threshold was set from $\Phi_c = 0.2$ to 0.05 whereas t was varied from 1.1 to 4. With increasing elongation of the carbon precipitates e.g. increasing t and decreasing Φ_c, the jump of conductivity at the percolation threshold decreases and the conductivity below the threshold e.g. in the tunneling regime, seems to be significantly higher compared to the regular particle morphology containing system. At lower temperatures, when the percolation network has not yet been formed or the carbon content is too small conduction is admitted by hopping of carriers among neighbouring particles or aggregates of carbon as it has been similarly described for carbon black- polymers (particle sizes in the range between 0.01 and 0.1 μm).[35] The t values obtained in carbon black filled materials are in good agreement with the value of $t \cong 2$ predicted by percolation theory whereas in short fiber filled composites t is much larger.

Adding additional filler materials with high conductivity such as metals or intermetallics offers the possibility to obtain composite materials of high conductivity even at low heat treatment temperatures (e.g. tunneling regime of the SiOC(H) matrix). For example poly(methylsiloxane) loaded with 40–60 vol% of $MoSi_2$ filler (mean particle size 2 μm, $\sigma_h \approx 5\times 10^2(\Omega cm)^{-1}$) was processed into heating elements which obtained a conductivity of 10^{-2} $((\Omega cm)^{-1}$ at 600°C and

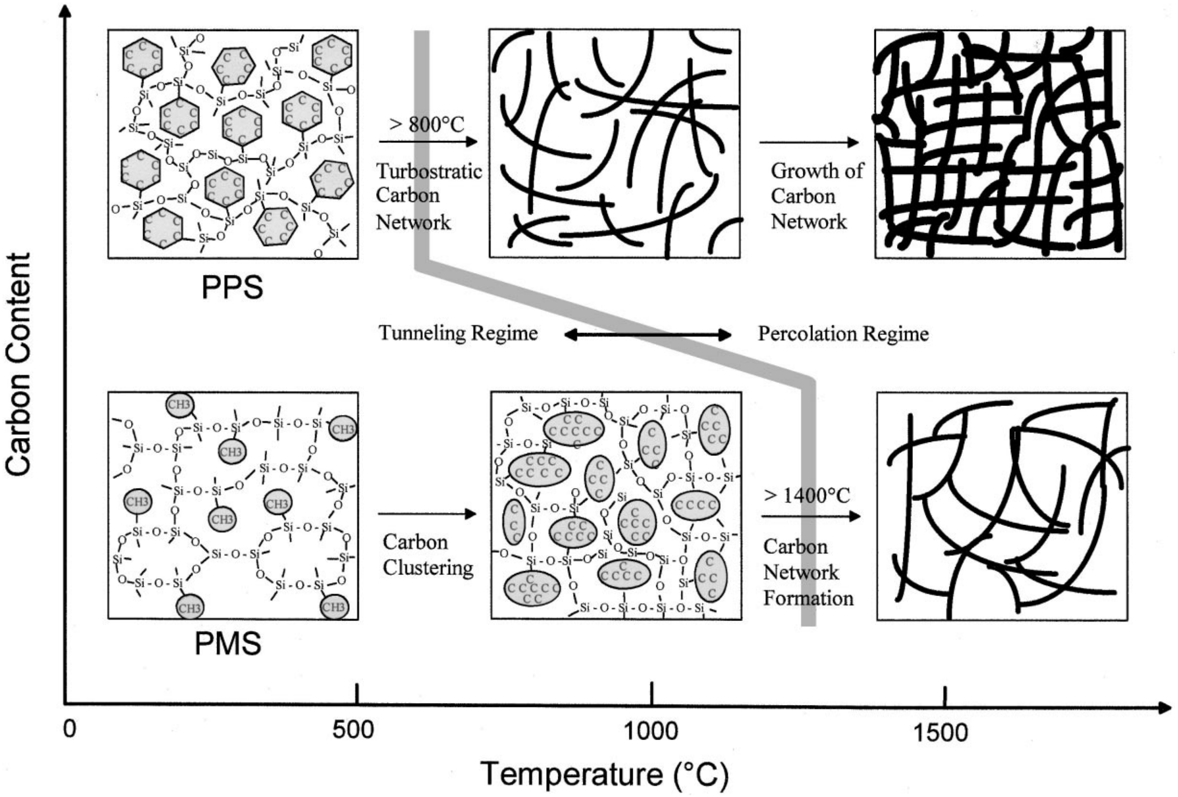

Fig. 10. Model of carbon redistribution reactions during pyrolysis in (bottom) PMS and (top) PPS derived ceramic residue.

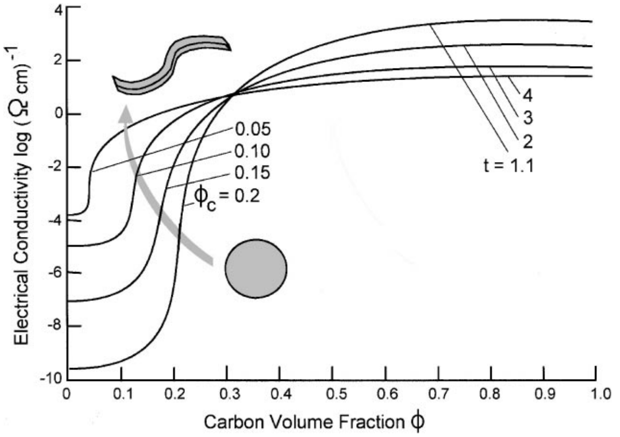

Fig. 11. Insulator-conductor precolation transitions calculated from Eq. (3) according to theory for different values of *t* and Φ_c.

10^4 (Ωcm^{-1}) at 1400°C.[31] The electrial behavior of the polymer/filler composite is dominated by the intrinsic filler conductivity, the morphology of the filler network and the particle/particle contacts. Due to the reaction of the filler with decomposition products of the polymer during pyrolysis ($7\ MoSi_2 + 12\ C \rightarrow Mo_2C + Mo_5Si_3 + 11\ SiC$) a complex nonlinear behavior is observed which gives rise for pronounced hysteresis of conductivity versus temperature (will be presented in a following paper).

5. Conclusions

Preceramic polymers have found increasing interest for the development of new ceramic materials and products. The thermal induced polymer to ceramic conversion (polymer pyrolysis) involves a complex series of microstructure transitions which may be examined by means of in situ electrical conductivity measurements. Depending on the carbon content in the polymer two different temperature regimes may be distinguished: at low temperatures ($<800°C$ PPS, $<1400°C$ PMS) semiconduction is attributed to tunneling of localized electrons (*tunneling regime*) whereas at higher temperatures a percolation network of precipitated turbostratic carbon provides electron conduction (*percolation regime*). Thus, kinetics of carbon precipitation and subsequent cluster growth are supposed to govern the electrical behavior of carbon bearing preceramic polymers upon heating. Tailoring of new polymer derived ceramics with respect to their electrical behavior should focus on the precipitation cluster dynamics. Using fillers which may react with carbon to form new carbide phases are, therefore, of particular interest to influence the carbon distribution. Fillers may additionally provide new functionalities such as improved strength, toughness, wear resistance, oxidation stability, etc. which are of particular importance when these new materials will be used in electrical and mechanical applications.

Acknowledgements

Financial support of German Science Foundation (DFG) under grant No. Gr 961/11 is gratefully acknowledged.

References

1. Rice, R. W., Ceramics from polymer pyrolysis, opportunities and needs-a materials perspective. *Bull. Am. Ceram. Soc.*, 1983, **62**, 889.
2. Wills, R. R. and Markle, R. A., Siloxanes, silanes, and silazanes in the preparation of ceramics and glasses. *Bull. Am. Ceram. Soc.*, 1983, **62**, 904.
3. Wynne, K. J. and Rice, R. W., Ceramics via polymer pyrolysis. *Ann. Rev. Mat. Sci.*, 1984, **14**, 297.
4. Peuckert, M., Vaahs, T. and Brück, M., Ceramics from organometallic polymers. *Advanced Materials*, 1990, **2**, 398.
5. Riedel, R., Seher, M., Mayer, J. and Szabo, D. V., Polymer-derived Si-based bulk ceramics, Part I. Preparation, processing and properties. *J. Eur. Ceram. Soc.*, 1995, **16**, 703.
6. Bill, J. and Aldinger, F., Precursor-derived covalent ceramics. *Adv. Mater.*, 1995, **7**, 775–787.
7. Greil, P., Active filler controlled pyrolysis of preceramic polymers. *J. Am. Ceram. Soc.*, 1995, **78**, 835.
8. Jacubenas, K. and Marcus, H. L., Silicon carbide from laser pyrolysis of polycarbosilane. *J. Am. Ceram. Soc.*, 1995, **78**, 2263.
9. Solomon, I., Spin effects in amorphous semiconductors. In *Amorphous Semiconductors, Topics in Applied Phys*, ed. M. H. Brodsky. Springer Verlag, Berlin, 1979, pp. 189.
10. Mott, N. F., *Electronic Processes in Non-Crystalline Materials*, Oxford, 1979.
11. Haluschka, C., Untersuchung elektrischer Eigenschaften multinärer Keramiken in den Systemen Si–C–N und Si–B–C–N. PhD thesis TU Darmstadt, Shaker Verlag Aachen, 1998.
12. Eins, U., Bill, J. and Aldinger, F., Elektrische Charakterisierung amorpher Si–C und Si–C–N Keramik. In *Werkstoffwoche 1996, Tagungsband Symposium 7 Materialwissenschaftliche Grundlagen*, ed. F. Aldinger and H. Mughrabi. DGM Informationsgesell schaft Verlag, Frankfurt, 1997, pp. 663.
13. Monthioux, M. and Delverdier, O., Thermal behavior of (Organosilicon) polymer-derived ceramics. V: main facts and trends. *J. Eur. Ceram. Soc.*, 1996, **16**, 721.
14. Bouillon, E., Lanlais, F., Pailler, R., Naslain, R., Cruege, F., Huong, P. V., Sarthou, J. C., Delpuech, A., Laffon, C., Lagarde, P., Monthioux, M. and Oberlin, A., Conversion mechanisms of a polycarbosilane precursor into an SiC-based ceramic material. *J. Mater. Sci.*, 1991, **26**, 1333.
15. Bouillon, E., Mocaer, D., Villenauve, J. F., Pailler, R., Naslain, R., Monthioux, M., Oberlin, A., Guimon, C. and Pfister, G., Composition–microstructure–property relatioships in ceramic monofilaments resulting from the pyrolysis of a polycarbosilane precursor at 800–1400°C. *J. Mater. Sci.*, 1991, **26**, 1517.
16. Chollon, G., Pailler, R., Naslain, R., Laanani, F., Monthioux, M. and Orly, P., Thermal stability if a PCS-derived SiC fibre with a low oxygen content (Hi-Nicalon). *J. Mater. Sci.*, 1997, **32**, 327.
17. Renlund, G. M., Prochazka, S. and Doremus, R. H., Silicon oxycarbide glasses. Part I. Preparation and chemistry; Part II. Structure and properties. *J. Mater. Res.*, 1991, **6**, 2723.
18. Filsinger, D. H. and Bourrie, D. B., Silica to Silicon: Key Carbothermic Reactions and Kinetics. *J. Am. Ceram. Soc.*, 1990, **73**, 1726.
19. Yakima, S., Okamura, K., Shishido, T., Hasegawa, Y. and Matsuzawa, T., Joining of SiC to SiC using polyborosiloxane. *Bull. Am. Ceram. Soc.*, 1981, **60**, 253.
20. Hurwitz, F. I., Gyekenyesi, J. Z. and Conroy, P. J., Polymer derived nicalon/Si–C–O composites: processing and mechanical behavior. *Ceram. Eng. Sci. Proc.*, 1989, **10**, 750.
21. Strife, J. R. and Sheehan, J. E., Ceramic coatings for carbon carbon composites. *Bull. Am. Ceram. Soc.*, 1988, **67**, 369.
22. Lipowitz, J., Polymer-derived ceramic fibers. *Bull. Am. Ceram. Soc.*, 1991, **70**, 1888.
23. Pivin, J. C., Colombo, P. and Tonidandel, M., Ion Irradiation of Preceramic Polymer Thin Films. *J. Am. Ceram. Soc.*, 1996, **79**, 1967.
24. Colombo, P. and Modesti, M., Silicon oxycarbide foams from a silicone preceramic polymer and polyurethane. *J. Sol–Gel-Science and Technology*, 1999, **14**, 103.
25. Hurwitz, F. I., Heinemann, P., Farmer, S. C. and Hembree, D. M., Characterization of the pyrolysis conversion of polysilsesquioxanes to silicon oxycarbides. *J. Mater. Sci.*, 1993, **28**, 6622.
26. Lipowitz, J., Rabe, J. A., Frevel, L. K. and Miller, R. L., Characterization of nanoporosity in polymer-derived ceramic fibers by X-ray scattering techniques. *J. Mater. Sci.*, 1990, **25**, 2118.
27. Lux, F., Review: models proposed to explain the electrical conductivity of mixtures made of conductive and insulating materials. *J. Mater. Sci.*, 1993, **28**, 285.
28. McLachlan, D. S., Blaskiewicz, M. and Newnham, R. E., Electrical Resistivity of Composites. *J. Am. Ceram. Soc.*, 1990, **73**, 2187.
29. Hahn, B., Weissmann, R. and Greil, P., EPR-investigation of carbon distribution in SiOC-glasses. *J. Mater. Sci. Lett.*, 1996, **15**, 1243.
30. Wild, M. J. and Buhler, P., On the phase composition of polymethylsiloxane derived ceramics. *J. Mater. Sci.*, 1998, **33**, 5441.
31. Cordelair, J., Electrical properties of polymer/filler-derived ceramics, PhD thesis, University of Erlangen-Nuernberg, Department of Materials Science, FRG, 1999 (in German).
32. Monthioux, M., Oberlin, A. and Bouillon, E., Relationship between microtexture and electrical properties during heat treatment of SiC fibre precursor. *Comp. Sci. Technol.*, 1990, **37**, 21.
33. Belot, V., Corriu, R. J., Leclerq, D., Mutin, P. H. and Vioux, A., Silicon oxycarbide glasses with low O/Si ratio from organosilicon precursors. *J. Non-Cryst. Solids*, 1994, **176**, 33.
34. Bois, L., Maquet, J., Babonneau, F., Mutin, H. and Bahlout, D., Structural characterization of sol–gel derived oxycarbide glasses: 1. Study of the pyrolysis process. *Chem. Mater.*, 1994, **6**, 796.
35. Carmona, F. and Mouney, C., Temperature-dependent resisistivity and conduction mechanism in carbon black-filled polymers. *J. Mater. Sci.*, 1992, **27**, 1322.
36. Stauffer, D., *An Introduction to Percolation Theory*. Taylor and Francis, London, 1985.
37. McLachlan, D. S., An equation for the conductivity of binary mixtures with anisotropic grain structures. *J. Phys. C: Solid State Physics*, 1987, **C 20**, 865.
38. Carmona, F., Conet, R. and Delhaes, P., Piezoresistivity of heterogeneous Solids. *J. Appl. Phys.*, 1987, **61**, 2250.
39. Balberg, I., Tunneling and nonuniversal conductivity in composite materials. *Phys. Rev. Lett.*, 1987, **59**, 1305.
40. De Bondt, A., Froyen, L. and Deruyettere, A., Electrical Conductivity of Composites: A percolation approach. *J. Mater. Sci.*, 1992, **27**, 1983.
41. Ueda, N. and Taya, M., Prediction of the electrical conductivity of two-dimensionally short fiber composites by a percolation model. *J. Appl. Phys*, 1986, **60**, 459.